



Large-aperture Telescope Tracking Control Based on Time-synchronization Strategy

Yun Li^{1,2}, Yu Ye^{1,2}, Shi-Hai Yang^{1,2}, Ling-Zhe Xu^{1,2}, Jin Xu^{1,2}, Hai Wang^{1,2}, Zhuang-Zhuang Deng^{1,2,3}, Rui-Qiang Liu^{1,2,3}, Xiao-Jie Gu^{1,2,3}, and Bo-Zhong Gu^{1,2}

¹ Nanjing Institute of Astronomical Optics & Technology, Chinese Academy of Sciences, Nanjing 210042, China; shyang@niaot.ac.cn

² CAS Key Laboratory of Astronomical Optics & Technology, Nanjing Institute of Astronomical Optics & Technology, Nanjing 210042, China

³ University of Chinese Academy of Sciences, Beijing 100049, China

Received 2023 June 13; revised 2023 September 10; accepted 2023 September 27; published 2024 February 20

Abstract

A time-synchronization strategy for packetized transmission of target position about a large-aperture telescope observation control system has been proposed in this study. Compared with the existing telescope tracking strategy, the target position packing and sending strategy based on the time synchronization method proposed in this paper has the advantages of high stability and reliability. First, the telescope tracking observation control method was elaborated in this paper, including the motion pattern during telescope tracking. Then, the strategy for packetizes transmission of target positions based on time-synchronization is established and lists the detailed steps. Finally, the performance of the tracking strategy is verified using the 2.5 m telescope for the simulated uniform speed star and the blind-tracking fixed star HIP 31216, respectively. The test results show that the accuracy root mean square of the tracking strategy proposed in this paper is less than 0''.02 at 30 minutes, and the performance is much better than the design requirement of 0''.3. The most important advantage of this tracking strategy is that the telescope can guarantee normal tracking for a certain period of time even if the hardware or software of the host computer is abnormal.

Key words: miscellaneous – telescopes – methods: observational – methods: analytical

1. Introduction

Telescopes have played a significant role in advancing our knowledge of astronomy and physics. They have enabled us to study celestial objects such as planets, stars, galaxies, and other cosmic phenomena that were once beyond our reach. In recent years, advancements in technology have led to the development of more powerful and sophisticated telescopes, such as James Webb Space Telescope (Gardner et al. 2006), Thirty Meter Telescope (TMT) (Weiss et al. 2020) and European Extremely Large Telescope (E-ELT) (Holzlöhner et al. 2022).

Telescope control systems are hardware and software programs that manage various aspects of telescope operation, such as pointing, tracking, and focusing. These systems are designed to automate tasks that would otherwise be time-consuming or impossible for astronomers to perform manually. Telescopes are often located in remote locations where weather conditions can be harsh, and the terrain can be challenging. In such cases, telescope control systems are essential as they allow astronomers to operate the telescopes from a remote location. As technology continues to advance, we can expect telescope control systems to become even more sophisticated, enabling us to explore the universe with greater precision and accuracy.

A reliable software platform can effectively improve the operational efficiency of equipment, such as the core Flight

System (cFS) proposed by McComas (McComas et al. 2016; McComas 2018). Researchers are trying to use it for telescope control software for ground-based and space-based observations (Park et al. 2022). The software system of the TMT consists of a software infrastructure called TMT Common Software (CSW) (Gillies et al. 2020) that interact with each other to satisfy the function of the various parts of the telescope, such as the pointing and tracking system and Alignment and Phasing System (APS) (Troy et al. 2016).

The performance of the telescope control system is directly related to the robustness of the control loop and the ability to avoid resonance excitation. E-ELT telescopes have defined new performance requirements for all engineering fields involved in the design and implementation of the telescopes (Marchiori et al. 2018; Colussi et al. 2020). To achieve reliable observation, Keck I and Keck II have implemented the Telescope Control System Upgrade (TCSU) project, which includes mechanical, electrical and software components (Kwok et al. 2018). To improve the tracking performance of Green Bank Telescope (GBT) (Ranka et al. 2016), a new method for identifying the correcting coefficients for encoder interpolation error is developed (Franke et al. 2015). The method reduced root mean square (rms) tracking error from 0''.68 to 0''.21. A quaternion-based solution using low-cost

hardware is proposed for rapid telescope pointing calibration (Riesing et al. 2018), it presented a quaternion-based pointing model for use with a star camera.

Model calibration to improve pointing accuracy is one of the commonly used methods. Imaging Atmospheric Cherenkov Telescope (IACT) improves tracking accuracy by means of pointing corrections made by a CCD camera capturing a Cherenkov camera with LEDs and an observational light source in the sky (Zhurov et al. 2019). GBT has developed a specialized pointing model to correct pointing accuracy for inaccuracies due to gravitational flexure, thermal deformation, azimuth track tilt, and offset errors (White et al. 2022). The Daniel K. Inouye Solar Telescope (DKIST) (Rimmele et al. 2020) and the Airborne Lunar Spectral Irradiance Mission (ALSIM) obtain lunar pointing (Newton et al. 2020) with the same improved accuracy through modeling. The quaternion-based pointing modeling method is an effective way to improve the pointing accuracy of telescope control systems (Riesing et al. 2018). In addition to model correction methods to improve pointing accuracy, iterative learning algorithms can also be used to address local pointing model inaccuracies and dynamic effects during tracking (Riel et al. 2019). Improving the accuracy of the telescope system with well-performing control models is also one of the commonly used tools, such as acceleration feedback control, which is effective in dealing with disturbances such as wind disturbances, nonlinear disturbances, and some other unknown disturbances (Wang et al. 2016).

In addition to software reliability, there are many other factors that affect ground-based telescope astronomical observations, such as distortions and instabilities (Rodeghiero et al. 2018), water vapor (Turchi et al. 2019), seeing (Parada et al. 2020), sites (Raymond et al. 2021). In addition to enhancing the performance of the telescope itself to improve the observation efficiency, new processing methods are also available. The method called digital tracking for asteroid searches that greatly increase the sensitivity of a telescope to faint unknown asteroids (Heinze et al. 2015).

Time synchronization strategies have wider applications in the field of astronomical observation and telescope control. The Main Atmospheric Cherenkov Experiment (MACE) telescope uses various subsystems such as a highly stable temperature-controlled oscillator clock synchronization Telescope drive Control Unit (TCU), an active mirror calibration system, camera electronics and signal processing based on the Global Positioning System (GPS) (Sarkar et al. 2017). The GTC telescope (Gran Telescopio CANARIAS) also plans to apply time synchronization methods to its distributed subsystems to improve system performance (Gaggstatter et al. 2016). The Cherenkov Telescope Array (CTA) improves the efficiency of acquiring high-energy gamma rays by synchronizing precise timestamps to distributed devices (Sanchez-Garrido et al. 2021). In addition to this, the concept of time synchronization

was introduced in telescopes for real-time tracking of satellites and satellite laser ranging in order to reduce the latency and at the same time reduce the problem of data loss (Seo et al. 2014).

This paper proposes a telescope tracking control method based on a time-synchronization strategy to achieve target position packing and transmission, which is more stable and fault-tolerant, and can ensure smooth progress of astronomical observation even when the TCS (Telescope Control System) and OCS (Observation Control System) host computers are abnormal. The method proposed in this paper can provides a new telescope tracking control strategy with higher tracking accuracy, greater stability, and fault tolerance.

The lack of a large-aperture optical/infrared telescope has seriously affected the development of Chinese astronomy, and the results of this research can provide technical support for next generation 10 m class telescope in China (Su et al. 2017).

The main strategies to improve the tracking accuracy of the telescope are: reducing the pointing tracking error of the control system itself, improving the accuracy of the pointing model, and the inclusion of the guide star system. In this paper, we start from reducing the pointing tracking error of the control system itself to improve the telescope tracking accuracy and enhance the reliability. The problem to be solved in this paper is to implement a tracking control strategy based on the time synchronization method for target position packing and sending to improve the accuracy and reliability of telescope tracking.

The novelties of the study are twofold:

1. The time synchronization strategy is a prerequisite for this research method, which utilizes a time server to synchronize the time of the OCS host computer, TCS host computer, and controller of the telescope control system, with an accuracy of milliseconds.
2. The target star position is packaged and sent to the controller. This research method can guarantee the normal operation of telescope astronomical observation in case of hardware or software failure of OCS and TCS computers, with high reliability and fault tolerance.

The rest of this paper is organized as follows: Section 2 presents the notion of telescope tracking observation control system, including the notion of drive system and tracking strategy presentation. Section 3 provides the theoretical background and implementation of method proposed in this paper. It also describes the application of Section 4 that describes the experiments developed according to the method in Section 3. Section 5 summarized the whole paper and details further research plans.

2. Telescope Tracking Observation Control

To achieve high-quality tracking observation of the target celestial body, the telescope needs to cooperate with the axis of azimuth, altitude and derotator. In addition, to capture clearer

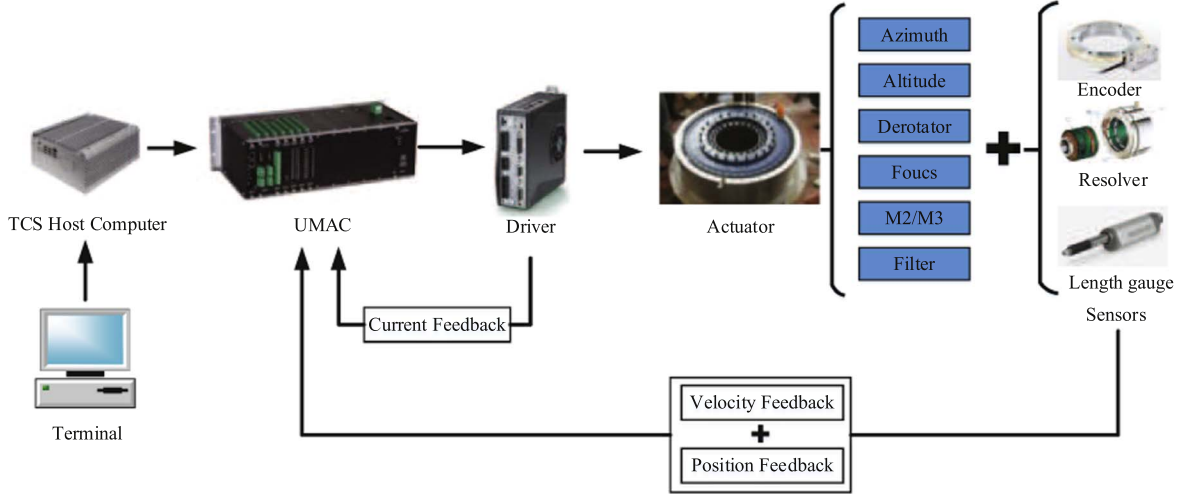


Figure 1. Telescope drive system schematic diagram.

images, systems such as focus adjustment, active optics, and adaptive optics are also involved. This paper only discusses how the telescope achieves precise tracking of the target celestial body.

2.1. Notion of Telescope Drive System

The drive system is the hardware and software foundation for achieving telescope tracking and observation, which includes TCS host computer, controller, actuators, sensors, and software processing programs. The control method adopts a multi-closed-loop control strategy, in which the main control computer sends instructions to the controller to drive the actuators to achieve azimuth, altitude, derotator, focusing, M2/M3 adjustment, filter and other motion mechanisms to cooperate with each other. Encoder, resolver and length gauge provide feedback information such as position and speed. The schematic diagram of telescope drive system is shown in Figure 1.

2.2. Telescope Tracking Observation Strategy

The essence of the process of tracking and observing a target star through a telescope from standstill is a pursuit problem. First, the Telescope Control System (TCS) calculates the position of the target star in the following period of time, and converts it into angular information in the three axes of telescope azimuth, altitude and rotation based on celestial coordinates. Then, the telescope moves from its current position in a high-speed pointing mode to the position of the target star. However, since the target star is also in motion during the pointing process of the telescope, the telescope also needs to adjust its pointing position. The process takes several iterations to complete to ensure a perfect encounter between the telescope and the target star at a certain time, before finally

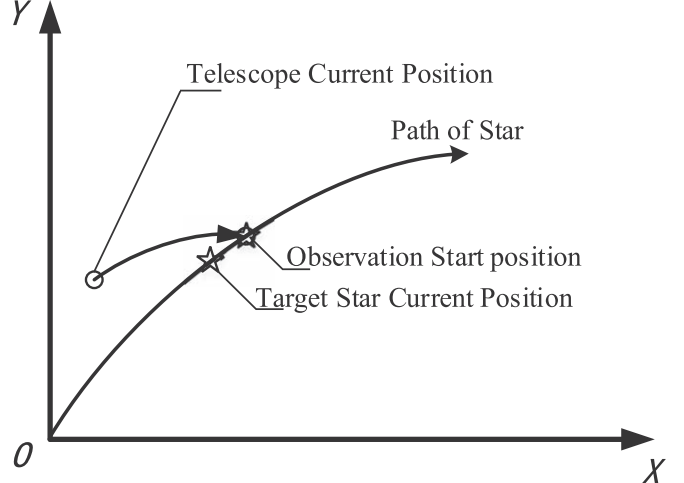


Figure 2. Telescope drive system schematic diagram.

entering the low-speed tracking phase. The schematic diagram of the telescope tracking observation is shown in Figure 2.

2.3. Motion Patterns during Telescope Tracking

In this paper, the telescope tracking observation process is divided into two parts: high-speed pointing and low-speed tracking. At the beginning of the design of the telescope, the maximum speed and acceleration during the pointing movement process, as well as the tracking error and other parameter indicators during the tracking process, will be determined. The maximum pointing speed is assumed to be $V_{\max}(\text{arcsec s}^{-1})$ and the acceleration is assumed to be $a_{\text{pointing}}(\text{arcsec s}^{-2})$ in this paper. The tracking speed is determined by the running speed of the target star.

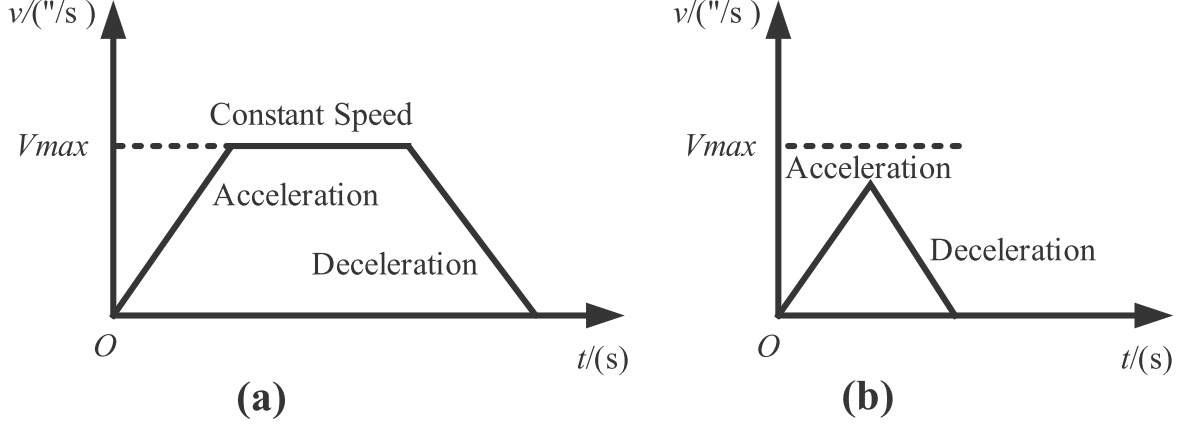


Figure 3. Schematic diagrams of motion mode 1(a) and motion mode 2(b).

The maximum velocity is one of the most important indicators of telescope design and is determined at the beginning of development. It is related to the rotational inertia of the telescope structure, the motor selection, and the size of the zenith blind zone. On the one hand, too small a maximum speed will lead to the inability to track the target near the zenith blind zone. On the other hand, too small a maximum speed will lead to the telescope's response speed is too slow, and the switching of the zenith zone is too time-consuming.

The high-speed pointing motion mode can be divided into two cases depending on whether the maximum speed is reached or not, and the two motion modes are determined by the critical distance of the telescope's current position from the target star's position. This critical distance can be calculated from the maximum pointing velocity V_{\max} and acceleration a_{pointing} , and it is set to S_0 . That is, $S_0 = 2 \times \frac{1}{2}a_{\text{pointing}}t_a^2$, where acceleration time $t_a = \frac{V_{\max}}{a_{\text{pointing}}}$. So, S_0 can be written as follows:

$$S_0 = \frac{V_{\max}^2}{a_{\text{pointing}}}. \quad (1)$$

Motion mode I: The pointing velocity reaches the maximum speed, which means that the pointing movement process is accelerated first, followed by a uniform speed, and then decelerated. At this time, the current position of the telescope is greater than S_0 from the target star position. In this motion mode, if the distance between the current position of the telescope and the position of the target star is S_x , the telescope pointing motion time T_x (second) can be calculated.

$$S_x = 2 \times \frac{1}{2}a_{\text{pointing}}t_a^2 + V_{\max}t_u. \quad (2)$$

Then, we can get the uniform motion time t_u ,

$$t_u = \frac{S_x}{V_{\max}} - \frac{V_{\max}}{a_{\text{pointing}}}. \quad (3)$$

So, the telescope pointing motion time $T_x = 2 \times t_a + t_u$ can be written as follows:

$$T_x = \frac{S_x}{V_{\max}} + \frac{V_{\max}}{a_{\text{pointing}}}. \quad (4)$$

Motion mode II: The pointing velocity does not reach the maximum speed, which means that the pointing movement process is accelerated first and then decelerated. At this time, the current position of the telescope is less than or equal to S_0 from the target star position. In this motion mode, the telescope pointing motion time T_x (second) can be calculated.

$$S_x = 2 \times \frac{1}{2}a_{\text{pointing}}t_x^2. \quad (5)$$

And then, we can get the uniform motion time t_x ,

$$t_x = \sqrt{\frac{S_x}{a_{\text{pointing}}}}. \quad (6)$$

So, the telescope pointing motion time $T_x = 2 \times t_x$ can be written as follows:

$$T_x = 2 \times \sqrt{\frac{S_x}{a_{\text{pointing}}}}. \quad (7)$$

The schematic diagrams of motion mode 1 and motion mode 2 are shown in Figure 3.

3. Theoretical Background and Implementation

3.1. Time Synchronization Strategy

The time synchronization strategy is the basis for the precise tracking observation method proposed in this paper for telescopes implementation. The time server can provide high-precision time services externally, such as the American GPS, the Chinese Beidou Navigation Satellite System (BDS), and

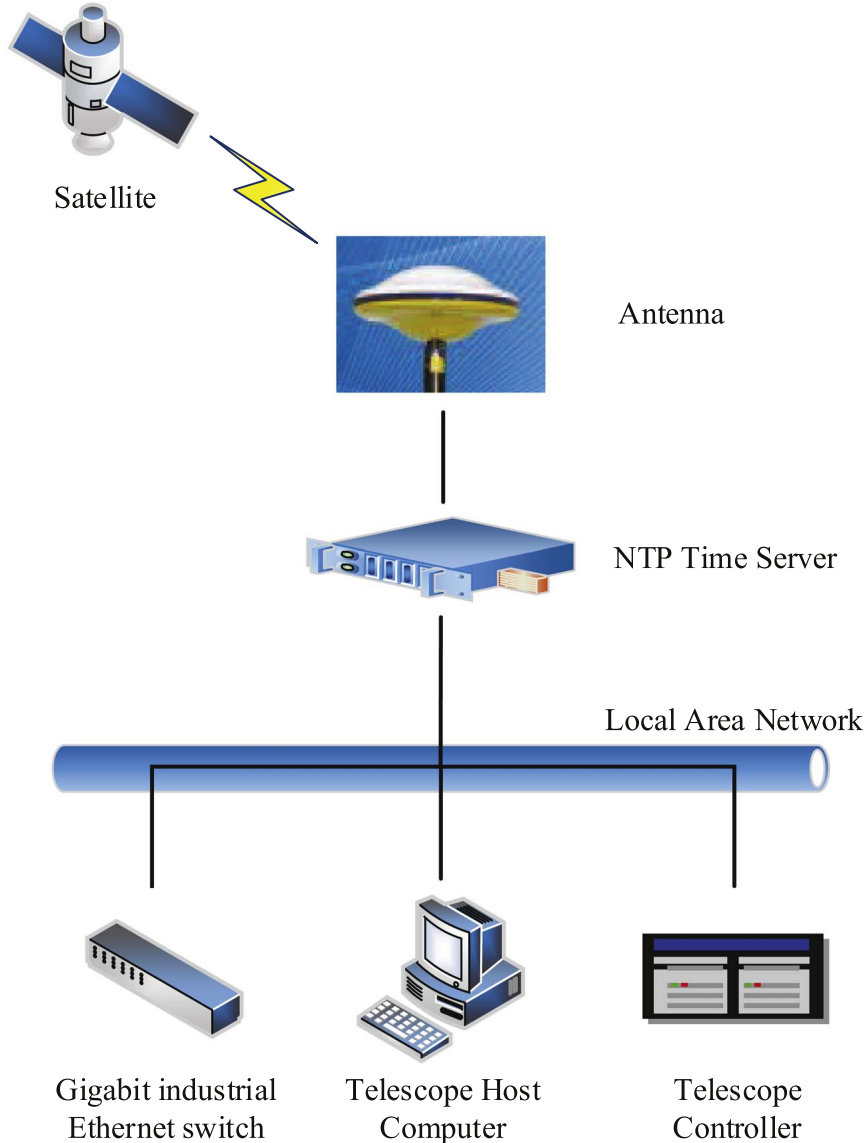


Figure 4. Schematic diagram of the time synchronization strategy.

atomic clocks. The calculation of the position of the target star, determination of the telescope pointing at the target, and the transmission of control instructions all rely on accurate time. Time servers regularly synchronize and calibrate the host computer and controller time of the telescope control system, with an error accuracy maintained at the millisecond level.

The time server, host computer and controller are connected via a fiber optic network through a Gigabit industrial Ethernet switch so that they work under the same Local Area Network (LAN). The time server provides Network Time Protocol (NTP) service to the host computer and controller. The schematic diagram of the time synchronization strategy is shown in Figure 4.

3.2. Target Location Packing and Sending

The target star position packing and sending are an important technical means for the telescope to realize the precise tracking observation method proposed in this paper, which is also based on the time synchronization strategy. The steps are as follows:

Step 1: For the observation of a known target star, the TCS host computer calculates the position of the target star and generates a catalog with a sampling interval of 100 ms. Each group of data contains time, azimuth position, altitude position and derotation position, which are recorded as Time, AZ_Position, ALT_Position and Dero_Position.

Step 2: The TCS host computer program reads the time of the first line of the star table, which is defined as

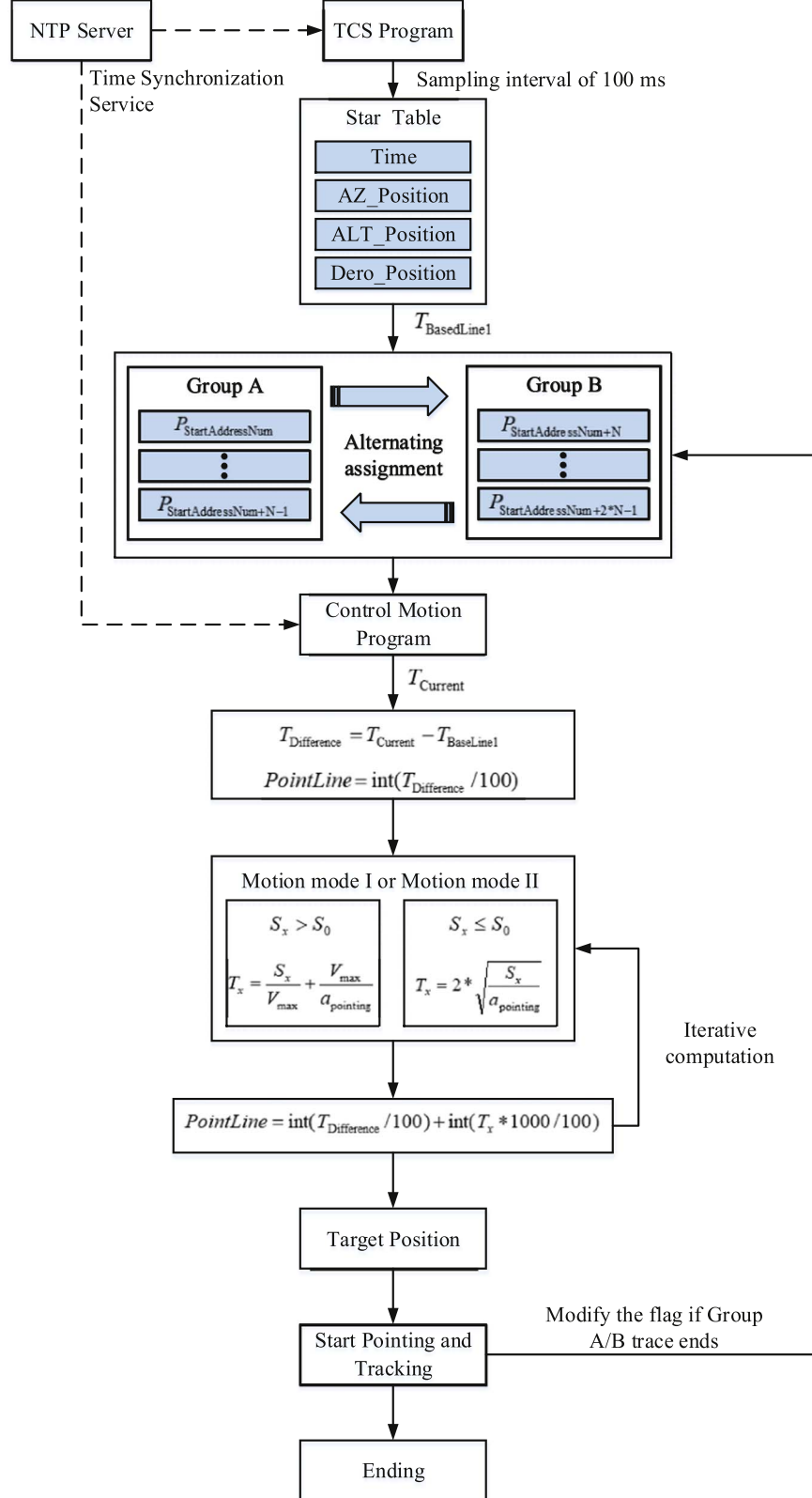


Figure 5. Schematic diagram of telescope tracking for target position packaging transmission.



Figure 6. The simulation (left) and physical (right) diagram of the 2.5 m telescope.

$T_{\text{BaseLine1}}$ (millisecond), and assigns the position data of the first line to N lines of the star table to the variables $P_{\text{StartAddressNum}} P_{\text{StartAddressNum}+N-1}$ in turn, where StartAddressNum is the P variable register start code, and the values of N and StartAddressNum are determined by the total number of controller registers. Then the above data is defined as group A and packaged and send to the controller of system.

Step 3: Same as step 2, the TCS host computer program assigns the $(N+1)$ th to (2^*N) th row of the star table position data to variables $P_{\text{StartAddressNum}+N} P_{\text{StartAddressNum}+2*N-1}$ in turn, then defines the above data as group B and sends it to the controller of system in package.

Step 4: Start the controller motion program while executing step 3, take the current time of the controller system, defined as T_{Current} (millisecond), and calculate the time difference between the current system time and first row of the star table time, defined as $T_{\text{Difference}}$ (millisecond). So,

$$T_{\text{Difference}} = T_{\text{Current}} - T_{\text{BaseLine1}}. \quad (8)$$

The number of rows in the star table at the current position of the target is defined as PointLine. That is,

$$\text{PointLine} = \text{int}(T_{\text{Difference}}/100). \quad (9)$$

Where $\text{int}()$ represents an integer function, commonly used in programming and mathematical expressions.

Step 5: The telescope should be pointed at the target location is defined as PointTarget, which is given by Equation (9),

$$\text{PointTarget} = P_{\text{StartAddressNum}+\text{PointLine}}. \quad (10)$$

The current position of the telescope is defined as CurrentPosition and is known. That is, the current distance

between target and telescope is,

$$S_x = |\text{PointTarget} - \text{CurrentPosition}|. \quad (11)$$

When $S_x > S_0$, motion mode I is executed, otherwise, motion mode II is executed. The pointing motion time of the telescope in different motion modes can be known from Equations (4) and (7). Update the value of PointLine, that is,

$$\text{PointLine} = \text{int}(T_{\text{Difference}}/100) + \text{int}(T_x \times 1000/100). \quad (12)$$

The value of PointTarget is also updated.

Step 6: Since the target star is not stationary during the pointing process of the telescope, and the velocity is not uniform. Therefore, when the telescope is pointing and moving to the target star position calculated in Step 5, the target star is no longer in this position. Theoretically, the pursuit problem requires repeated iterations of step 5 to complete, but countless iterations are not possible in engineering applications, so about 3 times is usually sufficient.

However, unlimited iterations are not possible in engineering applications, and the telescope have a certain field of view, so the number of iterations usually depends on the specific situation.

Step 7: From step 1 to 6, the precise position of the telescope should point to the target can be calculated, and the controller drives the telescope to point to the target. After completing the tracking of group A, it automatically switches to group B, then updates group A while tracking group B, and thus realizes the alternate tracking of two groups of data.

The schematic diagram of telescope tracking for target position packaging transmission is shown in Figure 5.

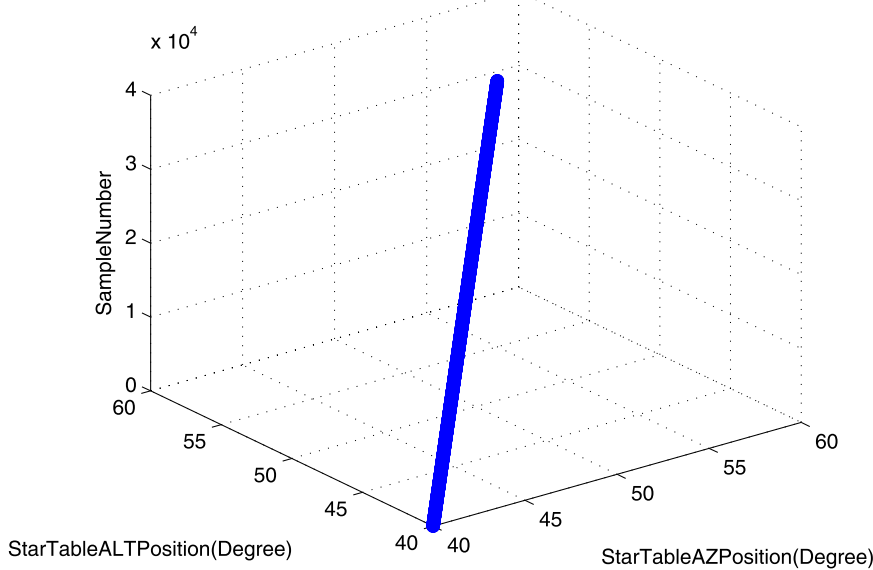


Figure 7. The orbital position of the simulated star.

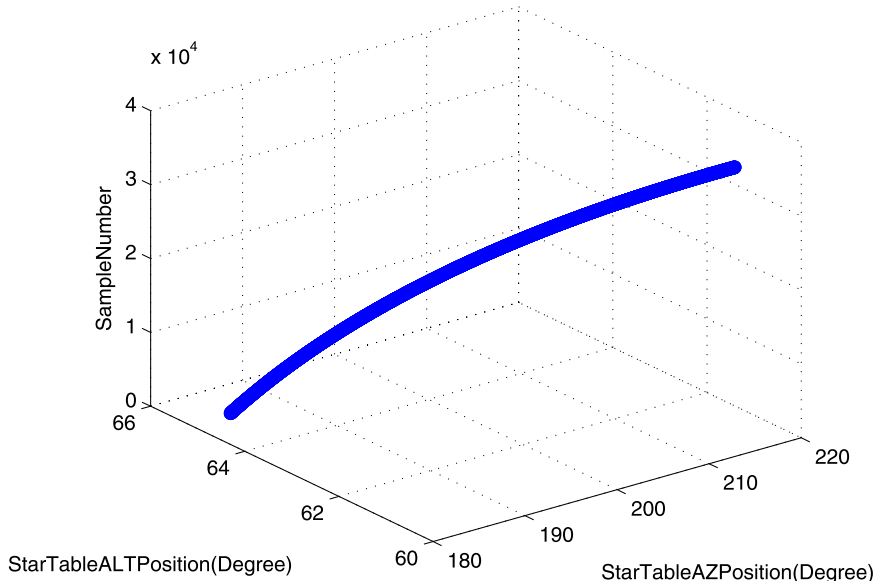


Figure 8. The orbital position of fixed star HIP 31216.

4. Performance Evaluation

4.1. 2.5 m Telescope Platform

The above content verifies the feasibility and advantages of the target localization packaging and tracking method based on time synchronization strategy proposed in this paper from the perspective of qualitative analysis. This section will prove it from the perspective of quantitative analysis.

A Chinese 2.5 m horizon telescope in the commissioning stage is the verification platform for this study, which is mainly used for observations of known target objects such as fixed stars and satellites. The azimuth axis inertia of the telescope is $12,400 \text{ kg m}^2$, and the altitude axis inertia is $32,000 \text{ kg m}^2$ during full load operation. The current state inertia is about 90% of the full load, which means that the current test can represent the performance of the telescope during observations.

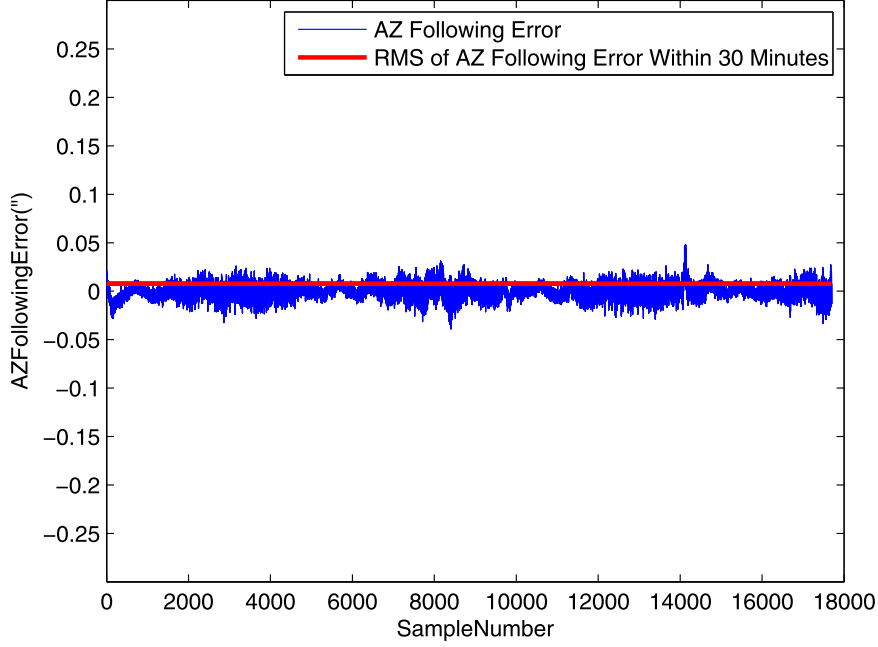


Figure 9. AZ following error and rms within 30 minutes of tracking the simulated star.

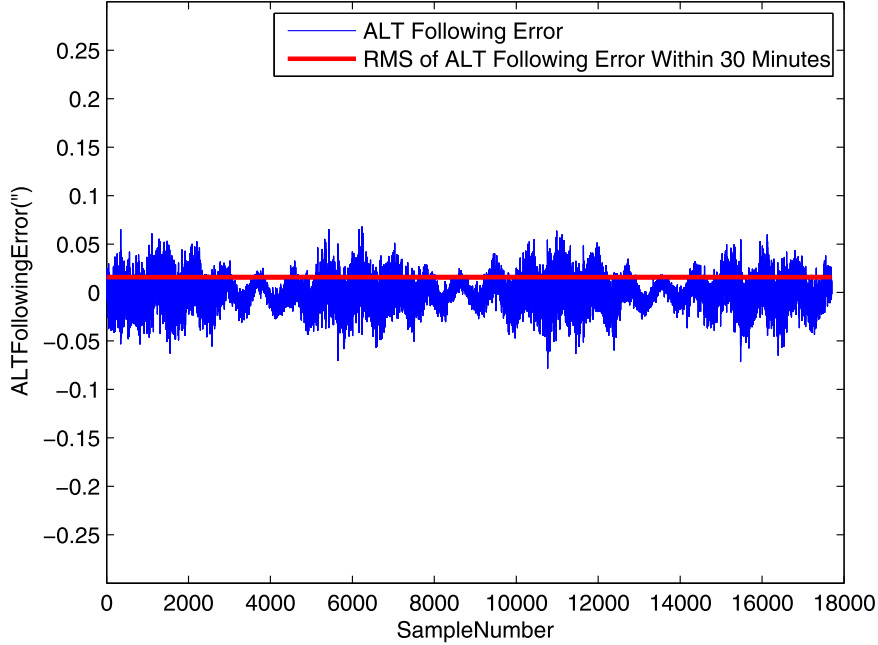


Figure 10. ALT following error and rms within 30 minutes of tracking the simulated star.

The simulation and physical diagram of the 2.5 m telescope are shown in Figure 6.

The control system of the telescope is mainly composed of host computer, controller, driver, motor and position feedback encoder. The resolution of the encoder is directly related to the tracking

accuracy of the telescope. The 2.5 m telescope of this research platform in this paper adopts a 29-bit absolute encoder with a resolution up to $0.^{\circ}0024$. Whereas the design specification for telescope tracking accuracy is $\text{rms} \leq 0.^{\circ}3$ with no guide closed loop, which is far more than adequate for the requirements.

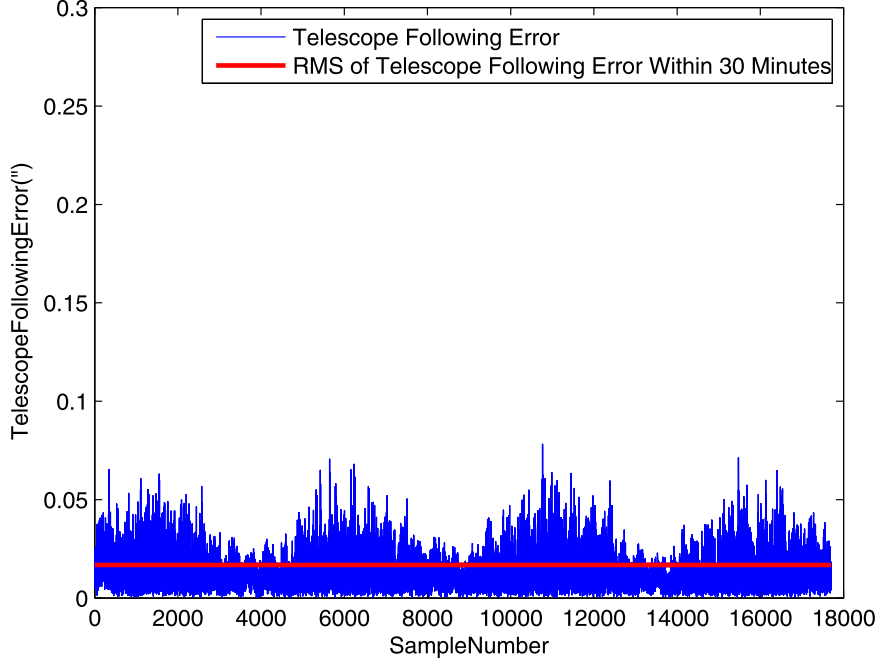


Figure 11. Telescope following error and rms within 30 minutes of tracking the simulated star.

Table 1
Information of Fixed Star HIP 31216

13 Mon—HIP 31216—SAO 114034 -HD 46300 -HR 2385	
Type:	Fixed star
Magnitude:	4.45
Absolute Magnitude:	-3.51
Ascension/decl.(J2000.0):	6 ^h 32 ^m 54 ^s .23 / 7° 19' 58"6
Ascension/decl.(Current):	6 ^h 34 ^m 09 ^s .14 / 7° 18' 58"9
Time angle/decl.:	0 ^h 14 ^m 15 ^s .83 / 7° 18' 58"9
Azimuth/Altitude:	189° 00' 07".8 / 66° 46' 48".8

4.2. Data Collection and Analysis

The 2.5 m optical telescope is currently in the commissioning phase. The frame of the azimuth axis and the main mirror compartment of the altitude axis have been installed, which can realize the simulation tracking of the target sky area.

The performance of the proposed tracking strategy is verified by using the 2.5 m telescope to track the simulated uniform speed star and fixed star HIP 31216, respectively. The trajectory of the simulated uniform speed star over an hour period is shown in Figure 7, with the telescope tracking at $15''\text{s}^{-1}$ for both the azimuth and altitude. The position of star HIP 31216 in the J2000 coordinate system is R.A.: $6^{\text{h}} 32^{\text{m}} 54^{\text{s}}.23$, decl.: $7^{\circ} 59' 58''6$ and its trajectory in one hour period is shown in Figure 8.

The purpose of tracking tests with telescope on simulated uniform speed star is to examine the performance of the telescope under long periods of uniform speed operation. The velocity of the simulated star in azimuth and altitude directions are $15''\text{s}^{-1}$, the starting position of the star table is AZ: $40^{\circ} 00' 00''$, ALT: $40^{\circ} 00' 00''$, and the current position of the telescope is at AZ: $10^{\circ} 00' 00''$, ALT: $20^{\circ} 00' 00''$. The telescope followed the simulated star for up to 30 minutes, and the following errors in azimuth and altitude are shown in Figures 9 and 10.

The tracking error of the telescope drive system can be known by combining the tracking error of azimuth and altitude using the coordinate system conversion equation, as shown in Equation (13)

$$\text{RmsTelescope} = \sqrt{\text{RmsAZ}^2 \times \cos^2\left(\text{TargetALT} \times \frac{\pi}{180}\right) + \text{RmsALT}^2}. \quad (13)$$

In Equation (13), RmsTelescope represents the tracking error of the telescope drive system, while RmsAZ and RmsALT represent the following error of azimuth and altitude, respectively. TargetALT denotes the target position of altitude. The tracking error of the telescope drive system followed the simulated star is shown in Figure 11.

To verify the real tracking performance of the tracking strategy proposed in this paper, fixed star HIP 31216 is

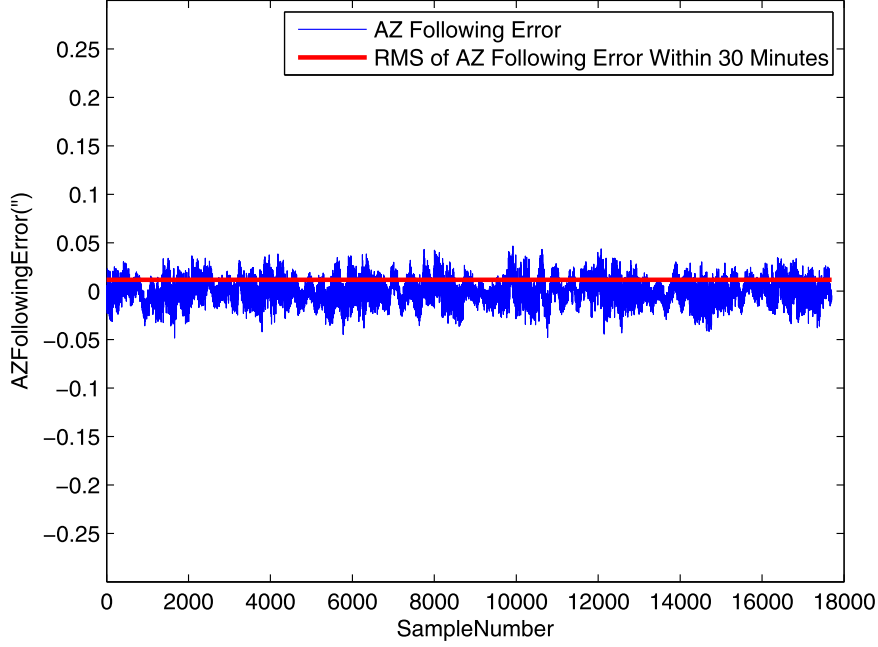


Figure 12. AZ following error and rms within 30 minutes of tracking fixed star HIP 31216.

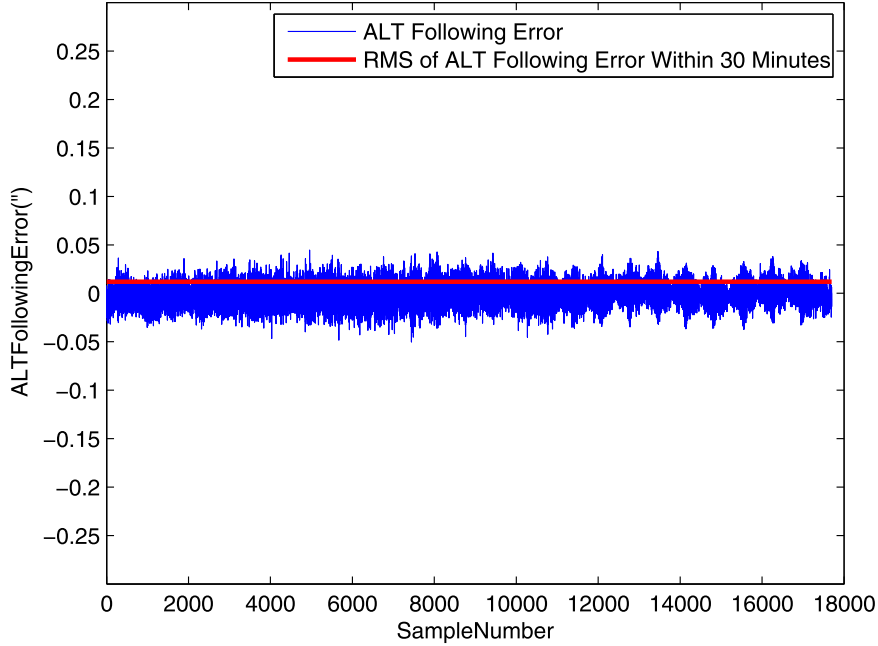


Figure 13. ALT following error and rms within 30 minutes of tracking fixed star HIP 31216.

randomly selected with the help of Stellarium software and blindly followed by the 2.5 m telescope, the detailed information of star HIP 31216 is shown in Table 1.

The telescope followed HIP 31216 for up to 30 minutes, and the following errors in azimuth and altitude are shown in

Figures 12 and 13, and the tracking error of the telescope drive system is shown in Figure 14.

The results of the quantitative calculations of the telescope azimuth, altitude and integrated tracking error are shown in Table 2.

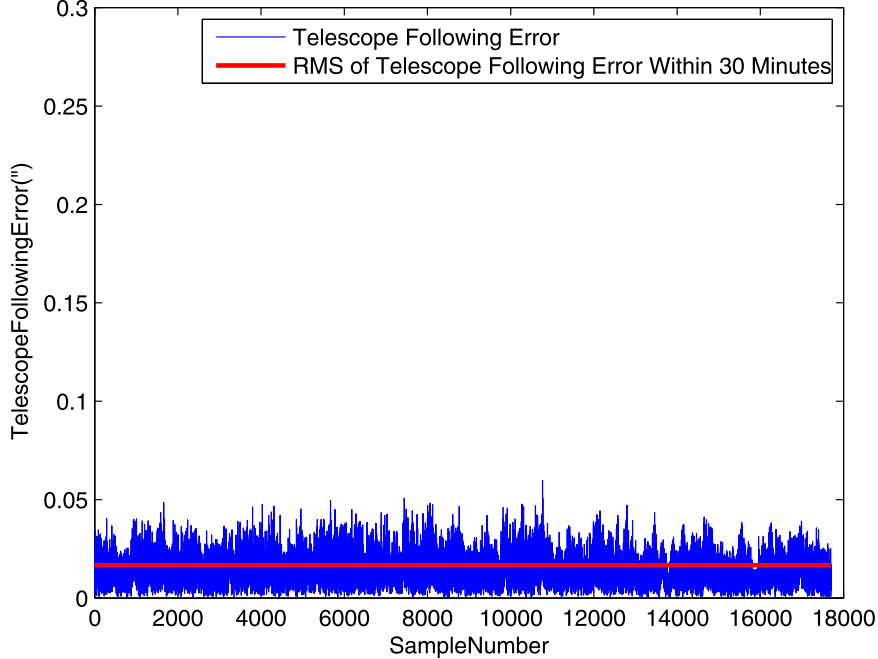


Figure 14. Telescope following error and rms within 30 minutes of tracking fixed star HIP 31216.

Table 2
Rms Following Error in the Tests

Target	RMSAZ	RMSALT	RMSTracking
Simulate star	0.0077	0.0159	0.0168
HIP 31216	0.0118	0.0120	0.0167

4.3. Explanation of Results

The design index of the tracking error rms about the 2.5 m telescope used for testing is $0.^{\circ}3$ with no guide closed loop. From the above results, it is clear that the error rms of the tracking strategy proposed in this paper is much better than the index requirement. The telescope tracking program stores 9000 position data in each group, meaning that the host computer sends 9000 position data to the controller at once. This behavior will enable the telescope to meet 15 30 minutes of normal observation even in the case of software or hardware failure of the host computer. This case was also verified during the test, which is the biggest advantage of the tracking strategy proposed in this paper.

4.4. Advantages of this Tracking Strategy

Compared with existing tracking strategies, there are obvious advantages of the method based on time synchronization strategy to achieve packetized delivery of target locations

proposed in this paper. The advantages are mainly reflected in the following twofold:

1. The tracking method proposed in this paper can avoid frequent error corrections in the telescope tracking process, which directly improves the tracking accuracy and indirectly improves the image quality.
2. The tracking method proposed in this paper can reduce the number of interactions between the host computer with controller, and reduce the probability of telescope tracking failure caused by communication abnormalities. The program can still ensure normal tracking for a certain period of time in the case of hardware or software crash of the TCS host computer, which gains time for the TCS computer to restart, so it has high fault tolerance and robustness.

5. Discussion and Conclusion

Based on the above study, it can be concluded that the tracking strategy based on time-synchronized packetized sending of target positions effectively reduces the frequency of interaction between the host computer and the controller, and achieves to guarantee the tracking observation for a specific time period even in the case of abnormal host computer. The new tracking strategy proposed in this paper is of great significance to improve the observational reliability of the telescope and the observational efficiency.

Acknowledgments

Thanks for the project supported by the National Natural Science Foundation of China (grant Nos. 11973065 and U1931207) and Jiangsu Funding Program for Excellent Postdoctoral Talent (2022ZB449) to this paper. Authors gratefully acknowledge financial support from China Scholarship Council (No. CSC201904910254) and Chinese Academy of Sciences Public Study Abroad Fund (Lingzhe Xu). The authors also acknowledge the support of the engineers and technicians from the Nanjing Institute of Astronomical Optics & Technology, Chinese Academy of Sciences.

References

Colussi, M., Colussi, L., & Ninane, N. 2020, *Proc. SPIE*, 11450, 114500R
 Franke, T., Weadon, T., & Ford, J. 2015, *JATIS*, 1, 044005
 Gaggstatter, T.-D., Nunez-Castain, A., & Molgo, J. 2016, *Proc. SPIE*, 9906, 990657
 Gardner, J.-P., Weiss, J., & Subramaniam, A. 2006, *SSRv*, 123, 485
 Gillies, K., Weiss, J., & Subramaniam, A. 2020, *Proc. SPIE*, 11452, 1145205
 Heinze, A.-N., Metchev, S., & Trollo, J. 2015, *AJ*, 150, 4
 Holzlöhner, R., Kellerer, A., & Lampater, U. 2022, *JATIS*, 8, 021504
 Kwok, S.-H., Tsubota, K., & Krasuski, T. 2018, *Proc. SPIE*, 10704, 107040N
 Marchiori, G., Rampini, F., & De, L.-S. 2018, *Proc. SPIE*, 10705, 107052E
 McComas, D. 2018, *IEEE Aerospace Conf.*, 1, 8
 McComas, D., Wilmot, J., & Cudmore, A. 2016, in Proc. AIAA/USU Conf. on Small Satellites, IV (Salt Lake City, UT: Utah Univ.), 20160010300
 Newton, A., Cataford, A., & Maxwell, S.-E. 2020, *AcAau*, 176, 558
 Parada, R., Rueda-Teruel, S., & Monzo, C. 2020, *Senso*, 20, 13
 Park, J., Lee, J.-O., & Kim, J. 2022, *PASP*, 144, 1033
 Ranka, T., Garcia-Sanz, M., & Symmes, A. 2016, *JATIS*, 2, 014001
 Raymond, A.-W., Palumbo, D., & Paine, S.-N. 2021, *ApJS*, 253, 1
 Riel, T., Sinn, A., & Schwaer, C. 2019, *AcAau*, 164, 121
 Riesing, K.-M., Yoon, H., & Cahoy, K.-L. 2018, *JATIS*, 4, 034002
 Rimmeli, T.-R., Warner, M., & Keil, S.-L. 2020, *SoPh*, 295, 12
 Rodeghiero, G., Pott, J.-U., & Arcidiacono, C. 2018, *MNRAS*, 479, 2
 Sanchez-Garrido, J., Jurado, A., & Jimenez-Lopez, M. 2021, *IEEE*, 70, 2000314
 Sarkar, D., Chouhan, N., & Tickoo, A.-K. 2017, XXXV Meeting of Astronomical Society of India, 3, 6
 Seo, Y.-K., Rew, D.-Y., & Kirchner, G. 2014, *AdSpR*, 54, 8
 Su, D.-Q., Liang, M., & Yuan, X.-Y. 2017, *MNRAS*, 469, 4
 Troy, M., Chanan, G., & Michaels, S. 2016, *Proc. SPIE*, 9906, 99066A
 Turchi, A., Masciadri, E., & Kerber, F. 2019, *MNRAS*, 482, 1
 Wang, Q., Cai, H.-X., & Huang, Y.-M. 2016, *RAA*, 16, 8
 Weiss, J., Gillies, K., & Subramaniam, A. 2020, *Proc. SPIE*, 11452, 114520V
 White, E., Ghigo, F.-D., & Prestage, R.-M. 2022, *A&A*, 659, A113
 Zhurov, D., Gress, O., Sidorov, D., et al. 2019, *J. Phys.: Conf. Ser.*, 1181, 012045